

# AN INTEGRATED RFID–UWB METHOD FOR INDOOR LOCALIZATION OF MATERIALS IN CONSTRUCTION

SUBMITTED: November 2021  
REVISED: July 2022  
PUBLISHED: July 2022  
EDITOR: Bimal Kumar  
DOI: [10.36680/j.itcon.2022.032](https://doi.org/10.36680/j.itcon.2022.032)

**Hassan Bardareh, Ph.D. student**  
*Department of Building, Civil and Environmental Engineering, Concordia University, Canada*  
[hassan.bardareh@mail.concordia.ca](mailto:hassan.bardareh@mail.concordia.ca)

**Osama Moselhi, Professor**  
*Director of the Centre for Innovation in Construction and Infrastructure Engineering and Management, Concordia University, Canada*  
[moselhi@encs.concordia.ca](mailto:moselhi@encs.concordia.ca)

**SUMMARY:** A considerable body of literature exists on automated object localization and tracking of construction operations. While GPS-based solutions have been widely investigated in many studies for outdoor tracking of these operations, indoor tracking proved to be more challenging. This paper focuses on indoor material localization and investigates the use of two remote sensing technologies—ultra-wideband and radio frequency identification—and the integrated use of these technologies to leverage the benefits of each for a cost-effective and practical solution for location identification of materials on site. The developed method is based on an experimental study conducted in two phases. In the first phase, experiments are designed and performed to evaluate the accuracy of ultra-wideband for localization, as well as to determine the optimal output power for a hand-held radio frequency identification reader. The optimal power is identified by evaluating the range measurement accuracy and maximum reading range of the hand-held radio frequency identification reader. In the second phase, the integrated use of radio frequency identification device and ultra-wideband for object localization is studied, and an improved trilateration technique is developed. The results of the experiments show an absolute error of 0.52 m and 1.15 m for 2D and 3D localization, respectively. Accordingly, the integration of these two technologies eliminates the need for using a large number of radio frequency identification reference tags on site for indoor material localization. The method is expected to enhance automated material tracking on construction sites by improving the localization accuracy and providing a straightforward data acquisition protocol. The analysis of experimental data captured in a lab setting is also presented, demonstrating the advantages of the proposed method.

**KEYWORDS:** Radio frequency identification, Ultra-wideband, Trilateration, Range measurement, Object localization

**REFERENCE:** Hassan Bardareh, Osama Moselhi (2022). An integrated RFID–UWB method for indoor localization of materials in construction. *Journal of Information Technology in Construction (ITcon)*, Vol. 27, pg. 642-661, DOI: [10.36680/j.itcon.2022.032](https://doi.org/10.36680/j.itcon.2022.032)

**COPYRIGHT:** © 2022 The author(s). This is an open access article distributed under the terms of the Creative Commons Attribution 4.0 International (<https://creativecommons.org/licenses/by/4.0/>), which permits unrestricted use, distribution, and reproduction in any medium, provided the original work is properly cited.



## 1. INTRODUCTION

Automated localization and tracking of materials have been widely applied in the construction industry, including for timely progress reporting, inventory planning and management, and safety. An automated approach to these activities helps to overcome the limitations of traditional approaches to material localization and tracking, which are primarily based on manual data acquisition. Using an automated approach, a large number of objects related to various activities can be localized and tracked. Automation also allows us to track activities within a specific timespan to enhance project control on site (Montaser and Moselhi, 2014; Moselhi and Bardareh, 2020). Moreover, automated indoor object localization has many applications in the maintenance and operation phase, as it is capable of providing more accurate as-built information for 3D modeling of the indoor environment compared to the traditional approach (Montaser and Moselhi, 2014; Li and Chan, 2013). Recent studies have also investigated object localization applications for tracking of workers and equipment for the purpose of improving safety on construction sites (Huang et al., 2021).

Nevertheless, localization and accessing of on-site information can be challenging due to the dynamic nature of on-site operations, including material delivery and utilization. Furthermore, there are challenges associated with timely acquisition and management of the large volumes of data involved in scheduling, project execution, and cost management. The feasibility and economic aspects of object localization represent another area of concern, and indoor material management and localization are also identified as areas with great potential for improvement (Montaser and Moselhi, 2014; Moselhi and Bardareh, 2020; Li and Chan, 2013).

Many studies have investigated the use of remote sensing (RS) technologies to automate the localization and tracking of objects on site (Montaser and Moselhi, 2014; Moselhi and Bardareh, 2020; Li and Chan, 2013; Labant et al., 2017; Ibrahim and Moselhi, 2014; Seo et al., 2013; Jo et al., 2015; Akhavian and Behzadan, 2015; Andoh et al., 2012; Su et al., 2014; Yoo and Park, 2019; Kalikova and Krcal, 2017; Ta, 2017). This paper introduces a novel method in which ultra-wideband (UWB) and radio frequency identification (RFID) technologies are integrated to efficiently localize objects in an indoor environment, thereby mitigating the cost burden associated with UWB or GPS sensors for localization and tracking of a large number of objects on construction sites. Moreover, the integrated use of the two technologies provides more accurate localization information not only for 2D but for 3D object localization, which is essential for the successful implementation of building information modelling (BIM). In this study, a sample number of objects labelled using less expensive passive RFID tags are localized at the experimental level. This integrated system provides a more economical and accurate method for indoor material localization compared to existing methods described in the literature. The performance of the developed method for object localization is validated in a series of experiments on these technologies in a lab setting.

The experimentation carried out in this study encompasses two phases. In the first phase, the individual performance of RFID and UWB are assessed separately, and the performance of the RFID reader for range measurement is investigated for four output powers. Then, the developed method employing these two technologies in an integrated manner is evaluated. The less expensive RFID tags make it possible to localize many objects on site but at a much lower costs compared to similar systems available in the literature. The studies in the literature are mostly based on the individual use of technologies such as GPS or UWB for localizing the resources on-site, which makes using these technologies uneconomic. The results for the localization of ten different objects shows an error of approximately 0.5 m for 2D localization and approximately 1 m for 3D localization. These are notable results in that they confirm the accuracy and cost-effectiveness of using this integrated system for localizing a large number of objects on site.

## 2. LITERATURE REVIEW

The literature reveals that a wide range of RS technologies, such as GPS, RFID, and UWB, have been used in the localization and tracking of various objects on site. Moselhi and Bardareh (2020) studied a number of different RS technologies, looking at the capabilities, limitations, and applications of each. They found that these technologies are used primarily to overcome the limitations of the manual and labor-intensive techniques traditionally used for data acquisition on site. Huang et al. (2021) noted that these technologies are used to efficiently access information related to location and tracking of materials, workers, and equipment on site for safety and resource management purposes. However, most of the technology-driven location and tracking applications have been for outdoor tracking of materials using GPS (Li and Chan, 2013; Labant et al., 2017; Ibrahim and Moselhi, 2014; Seo et al.,

2013; Jo et al., 2015; Akhavian and Behzadan, 2015; Andoh et al., 2012; Su et al., 2014), and GPS is not suitable for indoor applications due to signal disruption or distortion. Furthermore, because of the wide range of materials and structural objects present in an indoor environment, there is a need for a system in which a large number of items can be tracked efficiently. In this regard, RS technologies have been successfully deployed in the acquisition of indoor localization information to enhance 3D modeling of objects (i.e., BIM), helping to improve construction progress reporting, maintenance, and building operation (Moselhi and Bardareh, 2020; Valero et al., 2016). The application of Wi-Fi, Bluetooth, and Bluetooth Low Energy (BLE) technologies for range measurement and localization of objects has also been investigated recently, although further investigation is needed to confirm the performance of these systems for accurate object localization and tracking (Moselhi and Bardareh, 2020; Yoo and Park, 2019; Kalikova and Krcal, 2017; Ta, 2017). Liang et al. (2015), meanwhile, investigated the integrated use of smart phones and BLE technology as a way of localizing people in an indoor environment.

The technologies mentioned in the literature operate primarily based on signal measurement techniques. For instance, range-based localization is usually based on trilateration and triangulation techniques in which the received signal strength index (RSSI), phase-based indicator, and time-of-arrival (TOA) are used to measure the range distance from a tagged object (Montaser and Moselhi, 2014; Moselhi and Bardareh, 2020). Montaser and Moselhi (2014) investigated the accuracy of the proximity and triangulation techniques for 2D localization of the RFID tags attached to objects, concluding that the triangulation technique has superior localization accuracy compared to other range-based measurement techniques. Su et al. (2014), meanwhile, developed a boundary condition trilateration technique for RFID tag localization that selects a combination of RFID reader locations in a boundary condition scenario. In their scenario, a tag was localized if it appeared on the boundary circle (which has a radius equal to the maximum reading range of the RFID device). The combinations with a location distribution exceeding the standard spatial dilution factor were selected as a way of achieving better localization accuracy. Li et al. (2019) evaluated the use of range-free techniques such as fingerprinting to localize RFID tags. In their technique, the position of the target tag was obtained based on the coordinates of dense reference tags, which were selected by means of database-matching. Researchers have also considered the use of optimization and machine-learning algorithms as a means of improving the localization information acquired by RS technologies. The use of these algorithms helps to filter the initial data and to achieve better estimation for range measurement and localization applications. For instance, Ibrahim (2015) used a particle swarm optimization (PSO) algorithm to enhance the path loss model achieved by a wireless sensor network (WSN) system for indoor object localization. Valero et al. (2016) used a machine-learning algorithm to estimate the distance of tagged objects by translating the signal strength received. They used a BLE system in which a combination of convolution neural network (CNN) and artificial neural network (ANN) was employed for localization of the BLE tags.

RFID technology has been used in this respect with great capabilities for automatic identification and tracking of tagged objects on site. It is applicable for both built facilities and during construction activities due to its Non-Line-of-Sight (NLoS) capability, wireless communication, and on-board data storage capacity (Li and Becerik-Gerber, 2011; Bhatia et al., 2019). In addition to identification-based applications, RFID technology has also been used for object localization (Montaser and Moselhi, 2014; Su et al., 2014; Cai et al., 2014; Maneesilp and Wang, 2012). The main methods for object localization using RFID include trilateration, triangulation, proximity, and scene analysis. The former two techniques have mainly been used for tag localization, while the proximity technique uses reference points, where localization is achieved by monitoring the proximity of the tags to each of these reference points. Scene analysis, meanwhile, uses algorithms such as  $k$ -nearest neighbors (KNN) or probabilistic methods to localize tagged objects based on the similarity between the signal received and prior location fingerprints collected from the environment.

In the range-based techniques mentioned above, the distance between a hand-held RFID reader and a tagged object is measured by converting received signal strength (RSS) values to an experimental range value. In a study by Montaser and Moselhi (2014), the application of RFID for indoor location identification of materials was investigated using a series of experiments. In this study, the roving RFID reader and tag locations were tracked using a path loss model and trilateration technique (Montaser and Moselhi, 2014; Moselhi and Bardareh, 2020). In another recent study, Wu et al. (2019) experimented with the use of RFID for construction equipment tracking. They developed a positioning algorithm based on differential RSS while investigating the effect of environment factors (i.e. the presence of metal and line of sight) and directional orientation between RFID tags and receivers on the localization accuracy.

UWB, as another technology that has been employed for object localization, is a real-time location system (RTLS) that functions in a similar manner to an active RFID system. It uses very narrow pulses of radio frequency waves within a wide bandwidth for communication between tags and receivers. Due to the advanced technology available in the UWB sensor domain for obtaining time measurements accurate to the nanosecond range, various positioning techniques, such as time of arrival (ToA) or time of flight (ToF), angle of arrival (AoA), time difference of arrival (TDoA), and RSS-based techniques, have been used to localize objects. Several researchers have investigated the use of these technologies for location identification of resources in construction. Most of these efforts have focused on real-time tracking of workers, equipment, and materials (in both indoor and outdoor environments) to improve productivity and safety on construction sites (Moselhi and Bardareh, 2020; Cheng and Venugopal, 2011; Siddiqui, 2014; Park and Cho, 2016; Masiero and Fissore, 2017). For instance, Shahi et al. (2015) used UWB tags to localize and track the activities associated with installation of the pipeline and plumbing system of a building to improve progress reporting of these operations. Moreover, other studies have investigated the effect of the UWB sensors' distribution geometry, employment of filters (e.g., Kalman Filter, particle filters, etc.), and the use of static reference tags to enhance the localization accuracy of these sensors (Cheng and Venugopal, 2011; Siddiqui, 2014; Jimenez and Seco, 2016; Xu and Shmaliy, 2018; Nurminen and Ardeshiri, 2015; Sun and Wang, 2020; Almeida, 2005; Zhu and Ren, 2016; Song and Tanvir, 2015; Razavi et al., 2012; Liang et al., 2015).

Studies have also been conducted investigating the integrated use of multiple RS technologies to overcome the limitations of the individual technologies and thereby achieve a more reliable system in which a large number of objects can be tracked and localized. Examples of integrated systems for outdoor tracking of objects include systems, for instance, in which an RTLS such as GPS is integrated with barcode and RFID. For example, Song et al. (2015) designed a low-cost integrated GPS–Barcode system to track materials in a storage yard. Technologies integrating GPS with RFID, meanwhile, have been shown to provide better performance for tracking resources on site comparing to the GPS–Barcode (Moselhi and Bardareh, 2020; Li and Chan, 2013; Su et al., 2014; Cai et al., 2014). Cai et al. (2014), for instance, used a system consisting of spatially distributed mobile RFID readers equipped with GPS technology to track a set of mobile RFID tags. The central function of their integrated technology was to find the location of the RFID reader using a GPS receiver and then determine the locations of other tags accordingly using the RFID system. In addition, boundary constraints were incorporated in their system to address the challenges associated with unknown tag-reader distance. However, their system may not be practicable for localizing a large number of on-site objects, since it requires roving around each tagged object. Motroni et al. (2021), on the other hand, combined RFID technology with other sensory technologies such as proprioceptive sensors for indoor vehicle localization. They investigated the use of passive RFID reference tags, along with sensor-fusion techniques, to improve indoor localization accuracy.

Based on the literature, the use of RFID as a standalone technology for localization is subject to a number of limitations. For instance, for situations in which a roving reader is being used, a high density of reference tags is needed (Montaser and Moselhi, 2014). Moreover, for situations in which stationary RFID receivers are being used, the target object must either be moving or be within the reading range of a stationary receiver, and this increases the number of the receivers required on site, and even so the localization accuracy achieved is only within the range of meters. The use of UWB or Bluetooth in standalone applications as an alternative to RFID, meanwhile, is not economical for localizing a large number of objects in an indoor environment. The relatively long processing time required for the localization of the tags is also identified as a primary constraint, especially in the case of 3D localization (Montaser and Moselhi, 2014; Moselhi and Bardareh, 2020; Maneesilp and Wang, 2012).

Table 1 provides a brief overview of the capabilities, limitations, and localization accuracy of RFID, UWB, and the integrated method developed in this study, along with a comparison of the approximate costs of each system (Moselhi and Bardareh, 2020). As can be seen, the operating cost of each of these systems is based on the current market prices of the sensors and devices used in this experimental study (Decawave, 2016; Technology Solutions, 2019). The UWB used in the experiment described herein, it should be noted, is an off-the-shelf and open-source evaluation kit. The cost of commercialized UWB systems available in the market is much higher, making the developed method a reasonable and economical option for object localization in indoor environments. Moreover, the integrated use of the RFID and UWB technologies allows for the benefits of both technologies to be leveraged while overcoming some of the limitations associated with the individual application of each.

Table 1. RS technologies for indoor material localization.

| Technology          | Capabilities  | Limitations   | Cost*  | Localization Accuracy   |
|---------------------|---|---|--------|---|
| RFID                | 1) Less expensive   | 1) Low localization accuracy  | \$800  | Down to a few meters  |
|                     | 2) Non-line-of-sight  | 2) Calibration difficulties   |        |   |
|                     | 3) Availability in market   | 3) Affected by multipath effect   |        |   |
|                     | 4) Batch readability of tags  | 4) Need for a roving surveyor   |        |   |
|                     | 5) Straight forward usage   | 5) Mostly usable for 2D localization  |        |   |
|                     |   | 6) The hand-held RFID reader should be triggered in almost direct sight to the tags |        |   |
| UWB                 | 1) Long reading range (up to 100 m) of the sensors  | 1) High cost  | \$50k  | Down to a few centimeters                                     |
|                     | 2) Less influenced by metal and high humidity   | 2) Multipath and radio noise effect in the case of metal occlusion                  |        |   |
|                     | 3) Relatively immunity to multipath fading  | 3) Degraded range measurement accuracy as distance increases                        |        |   |
|                     | 4) Reliable 3D localization even in harsh environment   |   |        |   |
| Integrated RFID-UWB | 1) Much less expensive comparing to UWB system  | 1) Data synchronization   | \$2.8k | Approximately 1 m (in 3D)<br>Down to a few decimeters (in 2D) |
|                     | 2) Suitable for localization of a large number of objects, considering the localization accuracy and cost | 2) Need for a roving surveyor   |        |   |
|                     | 3) No need for reference tags for localization of the hand-held RFID reader                               | 3) RFID tags affected by Multipath effect   |        |   |
|                     | 4) Straight forward usage   | 4) The RFID reader should be triggered in almost direct sight to the RFID tags      |        |   |
|                     | 5) Providing 3D localization information  |   |        |   |

\* Assuming the need for localization of 100 objects on site (values are in Canadian currency).

### 3. DEVELOPED METHOD

#### 3.1 Overview

The method developed in this study is based on experimental work carried out in two phases. In the first phase, a set of experiments is carried out on the UWB and RFID technologies separately. In phase 2, a set of experiments is conducted on their integrated use for 2D and 3D localization of objects. A schematic diagram of the developed method is illustrated in Fig. 1. The novelty of this research lies in the integrated use of RFID and UWB for efficient object localization in an indoor environment, as well as in the development of an improved trilateration technique. Given that it is not economically practical to use UWB as a standalone technology for localizing objects on site, combining UWB with the less expensive RFID to facilitate object localization is investigated. RFID, for its part, is challenged in that the RSSI varies over time, as well as in that it is highly dependent on the site environment, especially in the case of indoor sensory localization (Dong and Dargie, 2012). Not only that, another challenge is that there is no conventional formula available for accurately translating the RSS values to range values that is generically applicable to all use cases in different environments, and this results in low positioning accuracy (Ruiz and Granja, 2017). Moreover, a large number of RFID reference tags need to be used to localize roving RFID readers and tags when using RFID as a standalone technology for localization of objects in an indoor environment

(Cai et al., 2014). As such, these two technologies are integrated in this study to leverage the benefits of each in object localization.

Despite the wide use of GPS in outdoor applications, this technology does not perform well in indoor environments since GPS devices need to receive signals from satellites. Thus, UWB sensors are often used in lieu of GPS for localization purposes in indoor settings. In fact, various techniques have been developed for localization of RFID tags, most of them based on signal processing. Since a roving RFID reader with known locations is used in the present study, a range-based technique is used for localizing stationary tagged objects. For applications associated with the localization of moving targets such as workers and equipment, it should be noted, UWB sensors are typically used to provide real-time location information. However, in the present study, because the main focus is on localizing materials rather than workers, only the range-based technique is used for this purpose. For that, the joint use of an RFID reader and a UWB sensor is experimented to evaluate the range-based technique for localizing the objects tagged by the RFID tags.

In phase one, experiments on RFID and UWB are carried out to evaluate the localization and range measurement accuracy of the UWB sensors used in this study, and to determine the optimal output power of the hand-held RFID reader for improving the accuracy of the range measurement information provided by the RFID system. With respect to the experiment on the RFID system, path loss models for four output powers of the hand-held RFID reader are developed and compared to identify the optimal output power. This value is identified by considering the maximum reading range of the hand-held reader and the accuracy of the corresponding model. (This optimal value is helpful for applications associated with range measurement and proximity on construction sites.)

In phase two, less expensive passive RFID tags are used together with the UWB sensors for providing localization information concerning a given group of objects. For this purpose, a UWB sensor is attached to the roving hand-held RFID reader in order to localize it. In this way, with the location of the mobile RFID reader in hand, the RFID tags attached to a set of identified objects can be localized using a path loss model and a trilateration technique, as is explained later in this paper. The experiments conducted in a lab setting validate the developed method as a means of providing 2D and 3D information about the tagged objects.

As depicted in Fig. 1, to localize a set of passive RFID tags attached to target objects, we first need to know the location of the hand-held RFID reader roving on site. In this experiment, the location of the hand-held RFID reader is acquired and recorded using the UWB tag attached to it. For the purpose of this experiment, one UWB tag is sufficient for the localization of the hand-held RFID reader. Another piece of information required for localization of the RFID tags is the distance of the hand-held RFID reader from these tags based on a predefined time interval (1 s in the case of the experiment described herein). The path loss model calculates this distance by converting the received RSSI values to a corresponding distance. As such, with the location of the hand-held RFID reader and its distance from each tag in the desired time interval known, the trilateration circles can be drawn for each RFID tag, as shown in Fig. 1.

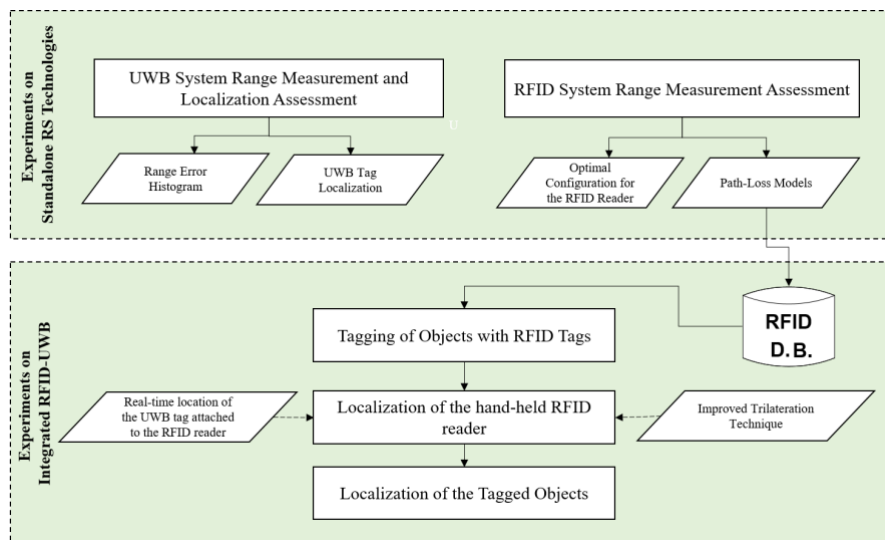


Fig. 1: Schematic diagram of the developed method for indoor object localization.

In order to localize an RFID tag in 2D, at least three circles are required. The location of the passive RFID tag attached to the target object is determined by finding the intersection of these three circles. Rather than rely on solutions to complex non-linear trilateration equations, a novel technique is implemented in this research in which a unified distribution of manipulated points is distributed over the area of each circle. Similarly, the manipulated point clouds are distributed in space for each sphere in 3D localization. As such, instead of solving the trilateration equation for 2D and 3D localization of each tag, the common points within the intersection space of the three circles (in the case of 2D) or the four spheres (in the case of 3D) are used for the localization of the RFID tag. A few different scenarios are considered in this study in order to ensure that the circles/spheres intersect properly. These scenarios include an incremental increase or decrease in the radius of the circles, if the circles are not intersecting or if the intersection area exceeds the predefined value. It should be noted that only the combinations of the three circles with the highest distribution around a given target object are selected for localization of that object. This practice has been shown in other studies to improve the localization accuracy of a GPS system (Xu and Shmaliy, 2018), and it is used in the present study to enhance the localization accuracy of the RFID system. Here, the combinations with the highest variance (in terms of their coordinates relative to a target tag or object) are selected for solving the trilateration equations. By applying these improvements to the trilateration technique, we achieve a 2D localization accuracy of 52 cm, while the corresponding value for 3D localization is 1.15 m.

### 3.2 Experimental setup

The experimental work is carried out over an area of 13 m × 8 m in an indoor environment (i.e., a lab setting). The area is divided into a grid of 90 cm × 90 cm cells as shown in Fig. 2.

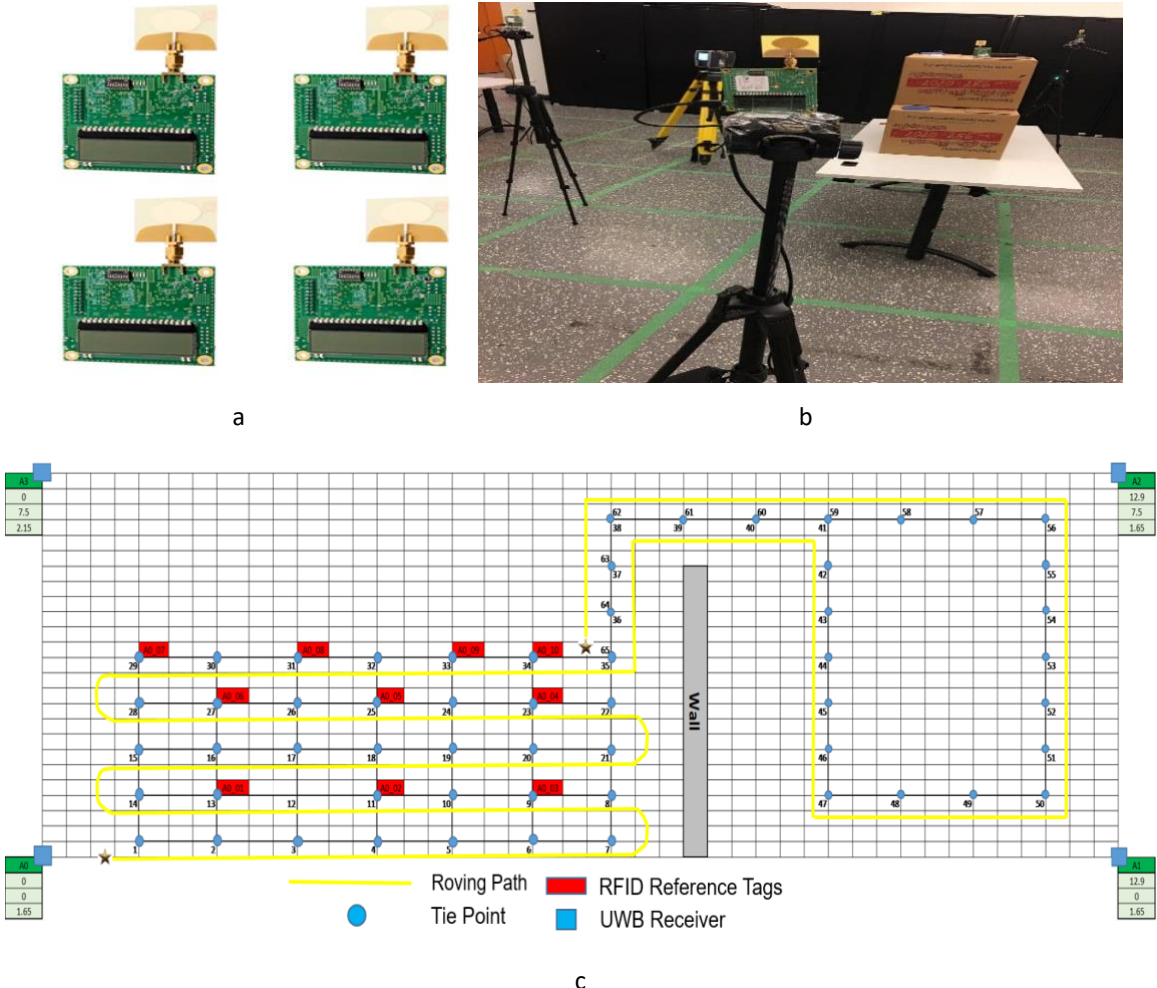


Fig. 2: Experiment environment. (a) UWB sensors (b) UWB receiver (c) Layout of the UWB sensors placement, RFID reference tags and tie-points.

The grid defines 65 ground-truth tie-points, including Line-of-Sight (LoS) and NLoS scenarios. Extending the tie-points to the NLoS scenario provides a means of evaluating the UWB system accuracy for scenarios in which obstacles such as walls and furniture may affect the localization accuracy. UWB receivers are located at each of the four corners of the area used for the experiments, and ten RFID tags are distributed around the area, as shown in Fig. 2. A fifth UWB sensor is affixed the mobile RFID reader. Of the four fixed UWB receivers, three are installed at a height of 1.65 m and the other at a height of 2.15 m. Installing one of the receivers at a different height allows the UWB system to localize the roving tag (mounted on the mobile RFID receiver) even for elevations above the height of the other three receivers. The roving UWB tag (i.e., the one attached to the mobile RFID reader) is at a height of 1.35 m. A series of three experiments is carried out: one on the UWB system, one on the RFID system, and one on the integrated system employing both technologies. These experiments are described in detail in sections 3.3, 3.4, and 4.1, respectively.

### 3.3 Experiment on the UWB system

The experiment on the UWB system consists of moving the mobile UWB tag along the path shown in Fig. 2 to rove over the 65 different ground-truth locations. A time interval of 30 s is considered for each tie-point, so each test lasts 32.5 minutes. The UWB system's data rate is set at 110 kbps on Channel 2 (3.993 GHz), which is the recommended configuration defined by the UWB manufacturer for longer-range measurements. The readings obtained in the 10 s before and after each displacement are removed from the dataset to guarantee sound ground-truth data. Under this configuration, three or four localization data points are recorded per second, which is a suitable level of granularity for real-time data acquisition. However, to increase the rate of data acquisition for the moving tags, a data rate of 6.8 Mbps is used. (The effect of the moving sensor on the localization accuracy of the UWB sensor is considered in the integrated RFID–UWB experiment based on the data acquisition protocol defined in section 5.) For further details concerning the experimental setup employed in the present study, the interested reader may refer to studies by Jimenez et al. (2016) and Ruiz et al. (2017), both of which used a similar set of experiments.

The UWB sensors employed in this study feature an atomic timer embedded in their PCB board that provides a high positioning accuracy (i.e., accurate to within a few decimeters). These are open-source sensors that can be purchased at approximately one eighth of the cost of commercial sensors, although they do not have a protected enclosure (Decawave, 2016). The purpose of the experimental work on these sensors is to investigate (1) the range measurement accuracy and (2) the localization accuracy of the UWB system.

To assess range measurement accuracy, the real-time ranging distance of the UWB tag from the stationary UWB receivers is measured. One way to improve ranging measurement is to remove outlier data from the estimation. Accordingly, in this experiment, any outlier ranging values in the NLoS scenario (i.e., readings with an absolute error deviating more than 0.8 m from the mean range error) in each stop are first removed from the raw data. Then, the ranging data points are split into three 5 m intervals (i.e., 0–5 m, 5–10 m, and 10–15 m). The ranging data obtained in the first and last 10 seconds of each stop having been removed as mentioned above, the distance of the roving tag from each receiver is determined by averaging the remaining ranging data (i.e., the data obtained in the middle 10-s interval) for each tie-point.

Fig. 3 shows the excellent performance of the UWB system under study, depicting the measured ranging values against actual ranging values. As expected, all data points are found to be above the diagonal line, which indicates the positive aspect of error due to the NLoS dispersion. In other words, the measured range values are found to be more significant than the actual values due to factors such as multipath effect and signal deviation.

Fig. 4 and Fig. 5 show the error histogram, mean range error, and standard deviation (SD) values in each ranging interval with and without omitting initial outliers in the NLoS scenario. Fig. 5 shows how removing outliers improves the mean ranging error, especially for longer-range intervals (notwithstanding the fact that it results in missing data for four of the 65 tie-points). For instance, in the third range interval (10–15 m), removing outliers results in an improvement of approximately 10 cm, while this improvement for the first range interval (0–5 m) is approximately 1 cm.

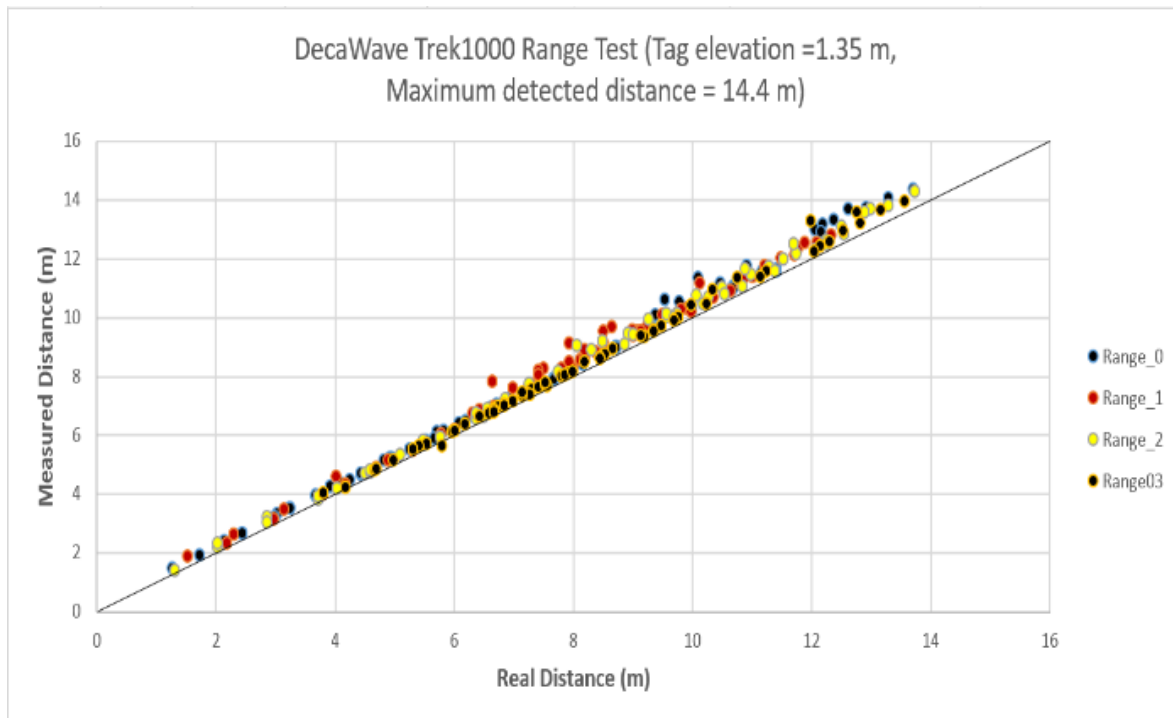


Fig. 3: Real versus experimental measured ranges.

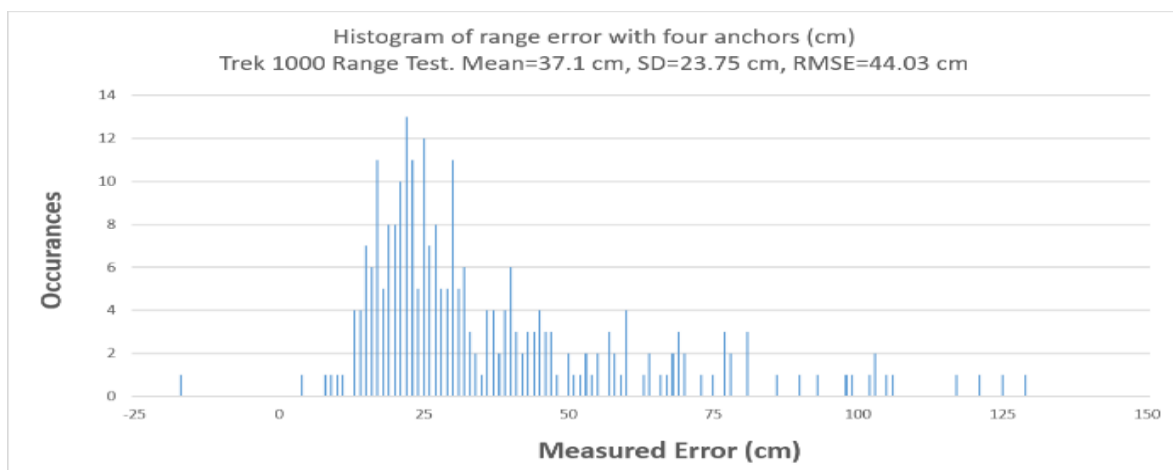


Fig. 4: Error histogram in NLoS scenario.

As for localization accuracy, the 3D localization information provided by the UWB is used to localize the hand-held RFID reader. For the interested reader, comparisons of existing methods for mitigating the localization error associated with NLoS or with scenarios in which these methods are employed are provided in studies by Jimenez et al. (2016) and Ruiz et al. (2017).

The results of the lab experiment on the UWB system show a Root Mean Square Error (RMSE) of approximately 20 cm for 3D localization. Meanwhile, the results for all 65 tie-points (i.e., without removing the outliers) show a 3D localization error of approximately 30 cm.

| Initial Mean Error and SD values |          |        |
|----------------------------------|----------|--------|
| Range                            | Mean (m) | SD (m) |
| 0_5                              | 0.2258   | 0.0915 |
| 5_10                             | 0.3259   | 0.21   |
| 10_15                            | 0.5216   | 0.256  |

| Mean Error and SD values without outliers |          |         |
|---|----------|---------|
| Range                                     | Mean (m) | SD (m)  |
| 0_5                                       | 0.2143   | 0.07311 |
| 5_10                                      | 0.3004   | 0.1426  |
| 10_15                                     | 0.4298   | 0.1752  |

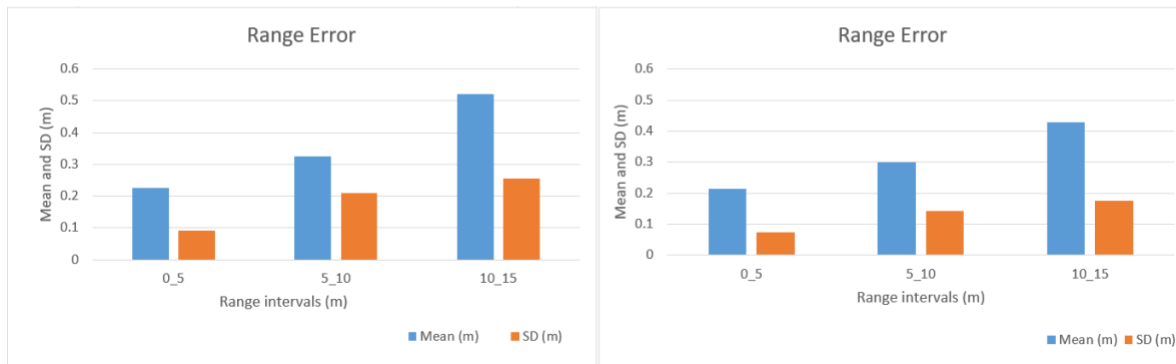


Fig. 5: Mean and SD error values with outliers (left), and without outliers (right).

### 3.4 Experiment on the RFID system

Various techniques are available for translating the distance between the hand-held RFID reader and the RFID tags. Most of these techniques are based on signal attenuation and depend on the characteristics of the given RFID system, such as the maximum reading range of the device (Montaser and Moselhi, 2014; Su et al., 2014; Cai et al., 2014). For the present study, an RSS-based method based on a path loss model is used for range measurement. However, various factors, especially factors associated with the particular RFID setup—such as operating frequency, output power of the hand-held RFID reader, and distance between the tags and the reader—may affect the accuracy of the measurements. In this regard, the results of a study by Shahi and Safa (2015) show that, if the distance between the reference tags is kept at half of the device reading range (0.5RR), then a better detection rate will be achieved. Factors associated with the indoor environment itself, meanwhile, such as the free space loss factor, multipath reflection, and interference effects, also influence the RSSI signal (Omer et al., 2019; Tzeng et al., 2008). Some of these factors are addressed and evaluated in this experiment to improve the ranging accuracy, which will be explained later through the following sections.

To obtain model for the range measurement, ten reference tags with known locations are located at select tie-points at a height of 1 m from the floor level (Fig. 2c). The model is developed for the RFID system based on a dataset of approximately 1,200 readings in each iteration of the experiment. Each resulting dataset, it should be noted, consists of tag reading times, tag IDs, and signal strength readings acquired while moving about the 35 tie-points in the LoS scenario. Fig. 6 illustrates the steps to obtaining the path loss models.

Four RFID reader output power levels are experimented with—020, 022, 025, and 029 decibel-milliwatts (dBm)—representing the minimum, conventional, proposed, and maximum outputs, and corresponding to Effective Radiated Power (ERP) values of 0.1 W, 0.16 W, 0.32 W, and 0.8 W. It is found that the maximum reading range of the RFID reader is increased by raising the output power of the reader. For each of these scenarios, after removing the data acquired in the first and last five seconds of each tie-point interval, the data points in the range that are less than the maximum reading range of the RFID reader are selected (i.e., the data points that are less than 3 m in the case of the 020 dBm scenario and those less than 6 m in the 025 dBm scenario). The initial regression line for each dataset having been obtained, the outliers with more than 1-m error are removed. Finally, the data is averaged at increments of 2 cm, resulting in the final regression model. Fig. 7 illustrates the path loss models for the four RFID reader outputs. The figure depicts the RSSI value versus the distance between the reference tags and the reader for each tie-point. Linear regression models are used for the present study. For an assessment of the various regression models that can be used for this purpose and their performance, the interested reader may refer to studies by Montaser and Moselhi (2014) and Razavi et al. (2012).

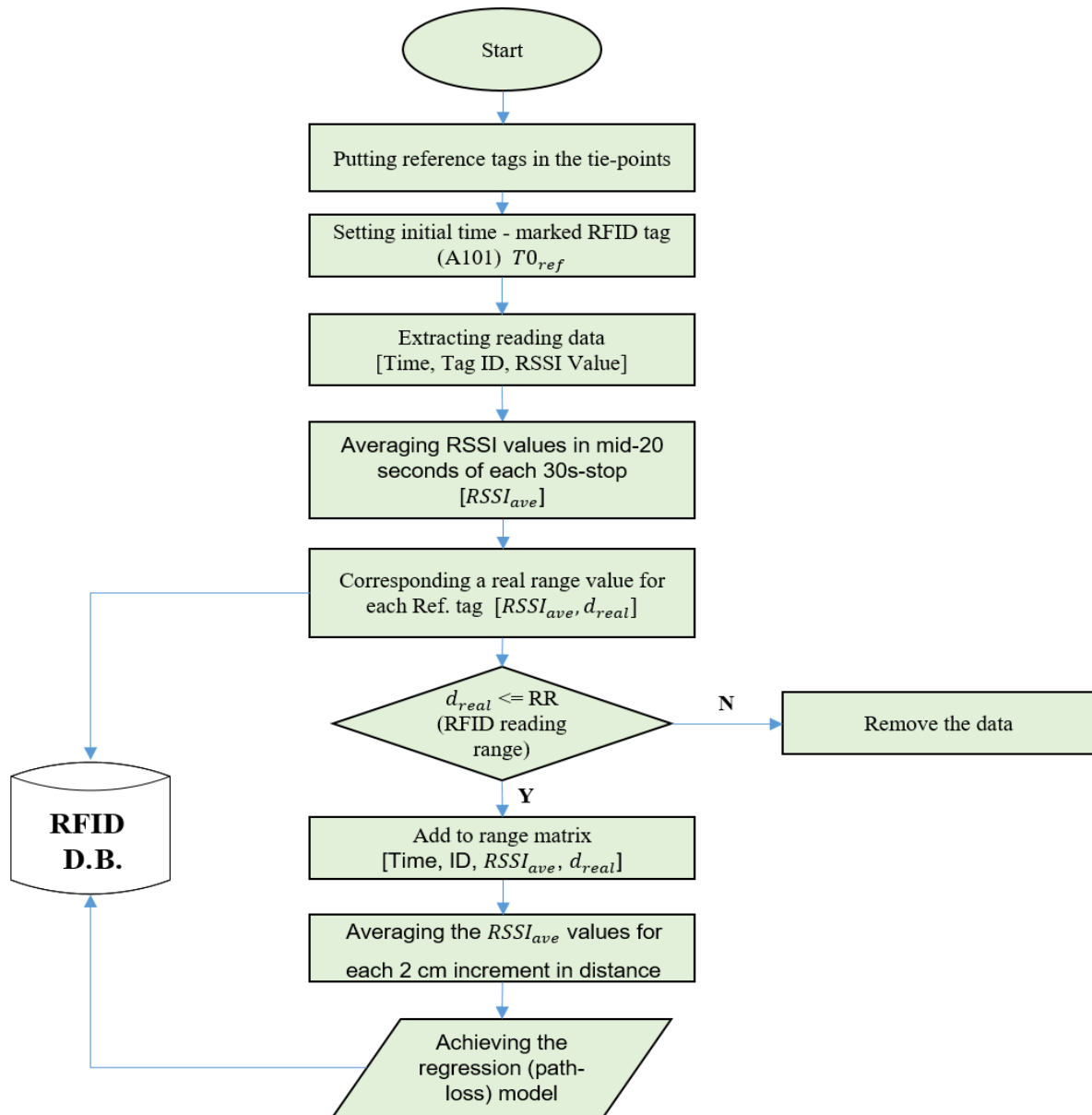


Fig. 6: Various steps to obtaining path loss models.

Table 2 shows the results for these scenarios, including the linear path loss equations used to obtain the distance range value (DRV), the  $R^2$  – value for each regression model, the maximum range of the RFID reader, and the absolute error in range measurement. Based on these results, the RFID system is found to perform best—in terms of the device’s maximum reading range and ranging accuracy—when the output is set to 025 dBm. This output is thus proposed for the range measurement applications (i.e., proximity warning systems) mentioned in the literature. Further investigation is needed to optimize the RFID output power by considering the two parameters, including the device’s maximum reading range and ranging accuracy. Other factors, such as the environment and multi-path effect, may bias the accuracy of the path loss models developed in this study which need more investigation in future.

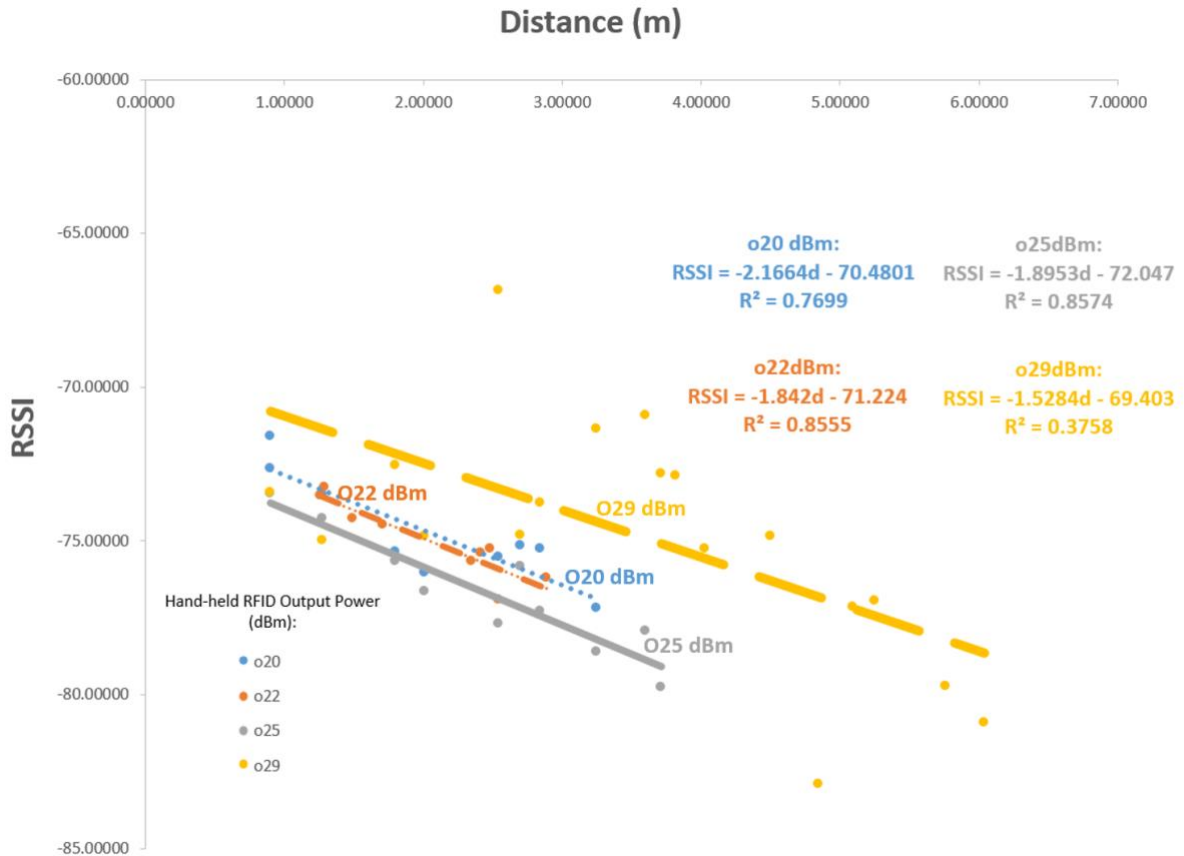


Fig. 7: RFID system path loss models.

Table 2. Results for path loss models.

| Scenario | Distance Eq.         | R <sup>2</sup> | Range (m) | Error (m) |
|----------|----------------------|----------------|-----------|-----------|
| o20 dBm  | -0.4616*RSSI-32.5333 | 0.77           | 3         | 0.79      |
| o22 dBm  | -0.5429*RSSI-38.6667 | 0.86           | 3.5       | 0.94      |
| o25 dBm  | -0.5276*RSSI-38.0135 | 0.86           | 6         | 0.91      |
| o29 dBm  | -0.6543*RSSI-45.4089 | 0.38           | 6.5       | 2.17      |

## 4. APPLICATION OF THE DEVELOPED METHOD

This section describes the data acquisition protocol, the integrated use of UWB and RFID, and the localization module.

### 4.1 Data acquisition protocol

The proposed protocol for data acquisition is based on the experimental work described above and is developed in consideration of the characteristics of each of the two technologies employed to enhance the localization accuracy. The data for evaluating the developed system is acquired in a manner similar to the procedure used in developing the path loss models for the RFID system as described above. However, in this case the UWB tag is used to measure the location of the hand-held RFID reader. Fig. 8a shows the device developed for this purpose, in which the UWB tag affixed to the top of the RFID reader provides the real-time location of the reader during data acquisition. Ten sample RFID tags are labelled and installed at a height of 1 m on the optional tie-points. One tag is designated as the time reference tag (A1\_01 in Fig. 8) for data synchronization purposes, with the acquisition of the RFID and UWB data being initiated when this tag is read in the Python code. At this juncture, a surveyor with

the hand-held RFID reader is prompted to begin roving in the lab; however, to enhance the accuracy of the UWB system in localizing the RFID reader, the surveyor stops moving when triggering the hand-held reader. At each stop, the RFID reader acquires the data from the RFID tags in the vicinity, depending on the maximum reading range of the reader (varying from 3 m to approximately 6 m). Since the surveyor moves arbitrarily in the lab, a time interval of 1 s is considered for the purpose of matching the RFID data with the UWB data, as this is the highest time resolution provided by the RFID reader.

For the experiments with the integrated RFID–UWB system, approximately 3,500 lines of data are acquired. This includes data for the three different RFID reader output power scenarios and for both 2D and 3D localization.

## 4.2 Integrated use of UWB and RFID

The integration of the acquired data and the mathematical concept developed to improve the range-based trilateration technique are described in this subsection. Based on the location of the RFID reader, the RFID tags are localized using signal processing together with a localization technique. Among the various RSS-based techniques for estimating tag locations, this experiment employs the DRV technique, with the DRVs being calculated using the path loss models as expressed in Equation 2. Using this equation, the constant values  $\alpha$  and  $\beta$  are obtained for the three RFID reader output power scenarios, i.e., 020 dBm, 022 dBm, and 025 dBm. In this study, as noted above, the 2D and 3D localization of the RFID tags is also investigated. The RFID tags are localized by replacing these range values in the trilateration equations (i.e., Equation 2).

$$\text{DRV} = \alpha \text{RSSI} + \beta \quad (1)$$

$$\text{DRV} = [(x_i - X_{r\_uwb})^2 + (y_i - Y_{r\_uwb})^2 + (z_i - Z_{r\_uwb})^2]^{1/2} \quad (2)$$

Where  $(X_{r\_uwb}, Y_{r\_uwb}, Z_{r\_uwb})$  is the location of the hand-held RFID reader, which is measured by the UWB sensor attached to it, and  $(x_i, y_i, z_i)$  are the coordinates of the target RFID tag (i.e.,  $i = 0, i = 1, i = 2,$  and  $i = 3$  for the four different RFID reader locations in 3D localization).

Since the tagged objects are static in this experiment, a small number of readers is sufficient for the localization of the tagged objects. However, in the case of localizing moving objects, a large number of RFID readers are required. To localize a tag in both 2D and 3D, combinations of the three (in the case of 2D) or four (in the case of 3D) reader locations in the data obtained for the given tag are selected for use in the trilateration equations for 2D and 3D localization. Since the selection of these combinations affects the localization accuracy, the combinations with the highest values of Spatial of Distribution (SoD) are given preference. It is worth mentioning that an increase in the number of selected data points for each tag dramatically increases the processing time of the localization module without significantly improving the localization accuracy. This is because all the combinations of the reader locations for each RFID tag should be selected from these data points. For instance, for 2D localization and assuming 10 readings for each RFID tag, 120 different statuses should be analyzed in the Python code for that tag (the factorial of selecting 3 from 10 options). However, a small number of combinations can also decrease the localization accuracy. For this reason, in this experiment the number of selected data points is two times of what is required for 2D and 3D localization (six and eight data with the highest SoD values, respectively).

The SoD value referred to here, it should be noted, is very similar to the value referred to within the domain of GPS as Dilution of Precision (DoP), which is used for enhancing localization in that domain. In fact, in GPS, localization accuracy will increase when visible satellites are far apart, resulting in a higher DoP value with a more robust geometry (Xu and Shmaliy, 2018). However, unlike in GPS, RFID does not operated based on clock offset (using the time difference to measure distance). In this respect, a novel approach that considers the effect of RFID reader locations on localization accuracy is needed. Accordingly, in this study, in a similar manner to the procedure for obtaining the DoP factor in GPS, the best combinations for the localization step are determined by calculating the mathematical variance of the various combinations of reader locations. Equation 3 expresses the SoD calculations used for selecting the initial data for the localization module.

$$\begin{bmatrix} S_x \\ S_y \\ S_z \end{bmatrix} = \begin{bmatrix} \frac{(X_1 - \mu_x)}{(n-1)} + \frac{(X_2 - \mu_x)}{(n-1)} + \frac{(X_3 - \mu_x)}{(n-1)} + \frac{(X_4 - \mu_x)}{(n-1)} \\ \frac{(Y_1 - \mu_y)}{(n-1)} + \frac{(Y_2 - \mu_y)}{(n-1)} + \frac{(Y_3 - \mu_y)}{(n-1)} + \frac{(Y_4 - \mu_y)}{(n-1)} \\ \frac{(Z_1 - \mu_z)}{(n-1)} + \frac{(Z_2 - \mu_z)}{(n-1)} + \frac{(Z_3 - \mu_z)}{(n-1)} + \frac{(Z_4 - \mu_z)}{(n-1)} \end{bmatrix} \quad (3-a)$$

$$\mu_i = \frac{(X_{i1} + X_{i2} + X_{i3} + X_{i4})}{4}; i = x, y, z \quad (3-b)$$

$$S^2 = S_x^2 + S_y^2 + S_z^2 \text{ (m}^2\text{)} \quad (3-c)$$

Where  $(X, Y, Z)$  are the RFID reader coordinates obtained by the UWB sensor,  $(S_x, S_y, S_z)$  represent the variance, and  $\mu_i$  is the mean value of the coordinates of the reader locations in each combination.

### 4.3 Localization module

As mentioned, the UWB tag provides information about the reader's location in the desired time span for locating the RFID reader. However, the UWB data are recorded at a millisecond time resolution ( $T_{uwb}$ ), whereas the RFID system records data at a time resolution of just one second ( $T_{ref}$ ). As such, first, the location of the hand-held RFID reader in each time span is obtained from the UWB tag affixed to it for 0.5 s before and after the time of the RFID tag reading time. Then, using the path loss models developed for the RFID, the range of the tagged object from the hand-held RFID is calculated accordingly.

Fig. 9 shows a diagram of the localization module in which an improved trilateration technique is developed to enhance the localization accuracy. At each passing second, information such as reference time, RFID tag ID, average RSSI for each tag, equivalent distance obtained from the path loss models, and RFID reader coordinates is recorded ( $T_{ref}, ID, RSSI_{ave}, d_{eq}, x, y, z$ ). The data is then rearranged based on the identified tag ID. The novelty of the developed trilateration module is that it defines an adoptive radius for the trilateration equations and considers the spatial distribution of the RFID reader locations in the localization module. These improvements help to compensate for the error in the RFID reader range measurements obtained from the path loss models, and they also aid in selecting the best combinations of the RFID reader locations for localization of each RFID tag. Meanwhile, by using distributed points in the trilateration circles, the need to solve non-linear and coupled trilateration equations can be avoided.

As mentioned above, in order to use trilateration equations for localizing a specific tag in 2D (or 3D), at least three (or four, in the case of 3D) readings of that tag are required. Each set of readings provides a unique combination with a specific SoD value for the RFID reader locations. In the initial step of the module and for data selection, data from the combinations with higher values of SoD are selected to be used in the trilateration equations. In the case of 2D localization, combinations of three out of six data, and, in 3D localization, combinations of four out of eight data, are selected.

For each combination, the three (four) circles (spheres) (defined by the location of the center of the circle in  $xyz$  coordinates) and a radius of  $d_{eq}$  are drawn, and uniform distributions of points are assigned to each circle (sphere). Here, a threshold value, or "ratio", is defined that is the ratio of the number of common points ( $n$ ) in the intersection of the selected circles (spheres) to the total points ( $m$ ) for each combination. If, by solving the trilateration equations (Equation 2), an intersecting area with an acceptable number of points is obtained (e.g., Ratio < 0.1), then the combination is accepted for the next step. However, if there is no intersection between the selected combinations (i.e., ratio = 0), or if the intersection area is too large (i.e., ratio > 0.1), then an incremental increase or decrease of the radius of the circles (spheres) is implemented to achieve the desired number of common points. These incremental increases and decreases in the radius of the circles (spheres) are defined in the extent of the ranging error of the path loss model for the identified optimal output power (025 dBm), which is approximately 1 m (Table 1). As such, a buffer of 50 cm inside and outside of the initial radius ( $d_{eq}$ ) of the circles (spheres) is considered, as this represents the extent of the error tolerance of the ranging measurement. Fig. 10a illustrates the concept of altering the radius of the circles for 2D localization.

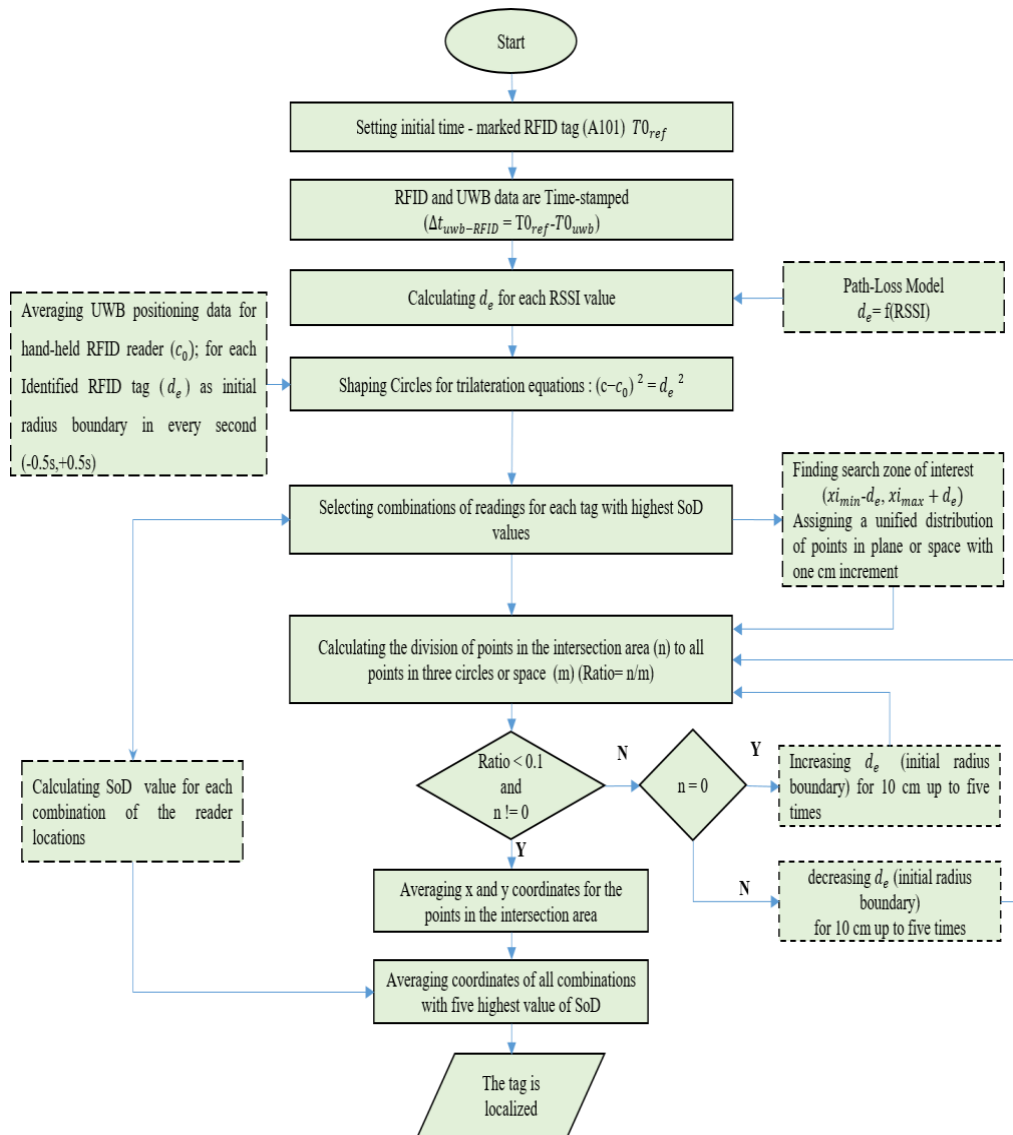


Fig. 9: System localization diagram.

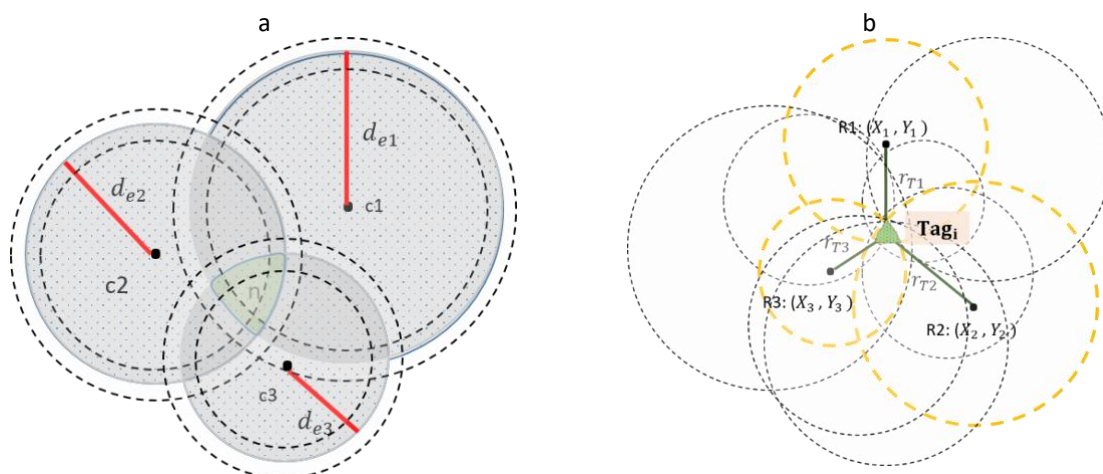


Fig. 10: Improved trilateration technique for 2D localization. (a) Radius variation in extent of the RFID system range measurement error (b) Combination with the highest SoD value (yellow dash-line).

In the final step of the module, those combinations with higher SoD values are used (Fig. 10b). As mentioned in the previous step, in this experiment the variance of the RFID reader location distribution in the lab is calculated to consider the effect of the geometry in localizing each RFID tag. Finally, the estimated location of each tag is calculated by averaging the coordinates of the points available in the intersection area.

## 5. RESULTS AND DISCUSSION

The results for various scenarios in which the RFID reader output is set to 020 dBm, 022 dBm, and 025 dBm are shown in Table 3. “Error1” refers to the localization error (in meters) before SoD analysis. “Error2”, meanwhile, shows the improved accuracy achieved after taking into consideration the spatial distribution of the reader in which the data with the highest values of SoD are selected and averaged.

Based on the results, an increase in the RFID reader output power decreases the localization accuracy; however, the maximum reading range of the device increases. This is in contrast to the finding of the experiments on the sole RFID device, in which 025 dBm is identified as the optimal output power for applications associated with range measurement: here the 2D localization error at an output power of 025 dBm is almost two times higher than the error at the conventional RFID reader output setting (022 dBm). This is because the developed 2D (3D) localization algorithm depends on the intersection of the circles (spheres). As the RFID output power increases, a larger area of plane (space) is occupied by the circles (spheres), and the localization algorithm capability to adjust the radius and control the ratio decreases. Moreover, the processing time of the algorithm dramatically increases at the optimal RFID reader output power level (025 dBm) identified in the previous experiment, especially for 3D localization.

*Table 3 Results of the various techniques for on-site material localization.*

| Technique       | RFID-UWB 2D Localization |             |                            | RFID-UWB 3D Localization | RFID (Montaser et al., 2014) | RFID-GPS (Hubo et al., 2014) |                           | RFID (Wu et al., 2019)    |
|-----------------|--------------------------|-------------|----------------------------|--------------------------|------------------------------|------------------------------|---------------------------|---------------------------|
|                 | Error 1 (m)              | Error 2 (m) | Confidence 95% for Error 2 | Error 2 (m)              | 2D Localization Error (m)    | 2D Localization Error (m)    | 3D Localization Error (m) | 2D Localization Error (m) |
| 020 dBm (< 3 m) | 0.48                     | 0.47        | 0.38–0.56                  | 1.04                     | 1.9 (+1.38)*                 | 2.48 (+1.95)*                | 2.59 (+1.44)*             | 1.25 (+0.73)*             |
| 022 dBm (<4 m)  | 0.65                     | 0.52        | 0.34–0.7                   | 1.15                     |                              |                              |                           |                           |
| 025 dBm (<6 m)  | 1.25                     | 1.01        | 0.32–1.7                   | 1.80                     |                              |                              |                           |                           |

\* *Improvement of the localization error in the developed method comparing to the previous studies.*

The results also show that the use of varying radius and SoD analysis does more to improve the localization accuracy when the reading range of the RFID reader is longer and when the output power is higher. Moreover, a longer RFID reader range entail that less surveying time and effort is needed for data acquisition. Using these techniques, the absolute 2D localization error improves to approximately 24 cm at 025 dBm, while the values at 022 dBm and 020 dBm are 13 cm and approximately 1 cm, respectively.

The developed method also shows good performance in the 3D localization of the tagged objects on site. For instance, in the case of the conventional RFID reader output power setting, the results show an RMSE of approximately 1.15 m. For comparison, as reported in the literature, the RMSE when RFID is deployed as a standalone technology and that when it is integrated with GPS are, respectively, 1.9 m and 2.59 m. As shown in the Table 3, by projecting the 3D localization information on the plane, the RMSE is shown to be approximately 0.52 cm for 2D localization, with a localization error of around 1 m in the elevation (z-axis). Comparing the localization error of the integrated method with that of the available UWB system, the error value of the developed method is over two times higher than that of the standalone UWB system. However, the cost of the developed method for object localization is much less than that of the individual UWB system. This is because less number of UWB sensors would be needed for object localization, while the localization accuracy is still in the range of a few decimetres. Table 1 provided the specifics for the cost and accuracy of the integrated system, compared to the standalone use of UWB and RFID.

It should be mentioned that the localization errors in Table 2 represent the cumulative error of the UWB system localization, RFID system path loss model, and the localization module, all of which affect the localization of the objects labelled with RFID tags. Techniques such as using particle filters or removing more outliers from the UWB localization data to enhance the localization data used for the RFID reader location could be explored in future

studies. Furthermore, a sensitivity analysis of the threshold values defined in the localization module, such as the ratio and the number of acceptable data with higher SoD values, may also improve the localization accuracy, though further investigation is needed to confirm this. The primary constraints for such an analysis would be the algorithm's long processing time and the computational effort required in order to solve the non-linear trilateration equations, especially in the case of 3D localization.

In the present study, a total of 15 2D and 3D localization scenarios are considered. This includes investigating the localization module under various ratio values and considering how this may affect the localization accuracy. Moreover, the effect of selecting a greater number of initial circles for solving combinations of the trilateration equations is also considered. However, it is found that, as the number of initial circles increases, the computational effort significantly increases, especially in the case of 3D localization. As a result of these analyses it is determined that the ratio value should be set to 0.1, while the number of initial circles for selecting combinations of circles for solving trilateration equations should be set to six and eight circles, respectively, for 2D and 3D localization. In future work, it would also be beneficial to investigate the effect of density of manipulated point clouds on the localization module's accuracy and processing time, especially for 3D localization. All these values have the potential to be optimized in future work by considering the localization accuracy and processing time required, both of which vary depending on the application.

The developed method provides object localization for indoor environments by taking advantage of low-cost RFID tags. In this way, a large number of objects can be localized without having to rely on extensive UWB or GPS sensing infrastructure (at a high cost). Besides, the integrated use of the UWB and RFID solves the problem of using a large number of RFID reference tags for localization of the roving hand-held RFID reader mentioned in the previous studies. In fact, instead of relying on a large grid of the RFID reference tags for localization of the hand-held reader, the UWB sensor attached to the reader can localize it each second. The integrated method developed in this study for indoor material localization can be easily extended to outdoor applications. For this purpose, long-range UWB or accurate GPS-based technologies could be used to localize the equipment and workers on site.

The investigation of the RFID system identifies the optimal output power for the hand-held RFID reader. Better performance for range measurement applications is achieved in terms of higher accuracy and longer reading range. Moreover, the developed trilateration technique improves the 2D and 3D localization accuracy of the RFID tags compared to the accuracy reported in previous studies.

## 6. SUMMARY AND CONCLUDING REMARKS

This paper investigates the possibility of localizing objects in an indoor environment by integrating two RS technologies, RFID and UWB, both of which have been individually applied in previous studies. The gaps identified in the literature point to the need for a system in which a larger number of objects can be tracked and localized in an indoor environment. The high cost of UWB sensors is the primary constraint limiting their use in such applications. The integrated use of UWB sensors with less expensive RFID technology is developed and experimented with in the present study to address this issue.

In the first step of the experiment, the performance of an off-the-shelf UWB system and an open-source hand-held RFID reader are evaluated. After assessing the accuracy of the UWB system for range measurement and localization, the experiments on the standalone RFID system provide models by which the distance of the RFID tags from the RFID reader can be calculated. This experiment also identifies the optimal RFID reader output power for range measurement applications. The conventional RFID reader output power (i.e., 022 dBm) is found to result in 94 cm absolute error for range measurement. The proposed optimal output identified in this experiment (i.e., 025 dBm), meanwhile, is found to have an error of approximately 91 cm, while the maximum reading range of the reader in the proposed output (approximately 6 m) is almost two times more than that of the conventional output.

The path loss models having been obtained, an improved trilateration technique is developed to localize objects labelled by the passive RFID tags. To achieve this, a UWB tag is attached to a hand-held RFID reader to localize it within each time span during data acquisition. After obtaining the RFID reader locations (defined as the centers of the circles), the path loss models are used to calculate the distance between the RFID reader and the RFID tags (i.e., the radius of the circles). By using trilateration equations with varying circle radii in the developed localization module, the 2D and 3D locations of the RFID tags are obtained. Moreover, the developed localization

module takes into consideration the effect of the spatial distribution of the reader location in order to enhance localization accuracy.

The localization method developed in this study is subject to three limitations corresponding to potential avenues of future study. (1) A long processing time is required for 3D localization of objects in higher ranges of RFID reader output. (2) Further investigation is required to improve the accuracy of range values for the trilateration equations. For this purpose, the use of innovative techniques such as machine learning and optimization to better calibrate the RFID and UWB devices, as well as the use of filters to improve the localization information, should be explored. (3) In the present study, the tagged objects are all located at the same height when evaluating the 3D localization capability of the developed method. To better assess the localization module, the RFID tags should be located at varying elevations. Besides, the accuracy of the developed method depends on path loss models obtained in each experimental environment. To obtain these, accurate positioning of the RFID reference tags in the tie-points is required. However, the auto-positioning and localization capability of the UWB system can also be used to localize RFID reference tags in the tie-points, though with less localization accuracy.

The localization information obtained by deploying the developed method can be used for daily progress reporting on various activities. For this purpose, the objects associated with each activity must be labelled by the RFID tags and localized. This information can also be used to better control inventory and improve supply chain management on site.

## REFERENCES

- Akhavian R. and Behzadan A.H. (2015). Construction equipment activity recognition for simulation input modeling using mobile sensors and machine learning classifiers, *Advanced Engineering Informatics*, Vol. 29, No. 4, 867–877.
- Andoh A.R., Su X., and Cai, H. (2012). A framework of RFID and GPS for tracking construction site dynamics, In *Proceedings of the 2012 Construction Research Congress: Construction Challenges in a Flat World*, West Lafayette, IN, United States, May 21–23, pp. 818–827.
- Almeida A. and Almeida J. (2005). Real-time tracking of moving objects using particle filters, In *Proceedings of the IEEE International Symposium on Industrial Electronics*, Dubrovnik, Croatia, Jun. 20–23, pp. 1327–1332.
- Bhatia A. P. (2019). Integrated System for Concrete Curing Monitoring: RFID and Optical Fiber Technologies, *Journal of Materials in Civil Engineering*, Vol. 31, No. 3, 06018028.
- Cai H., Andoh A.R., Su X., and Li S. (2014). A boundary condition based algorithm for locating construction site objects using RFID and GPS, *Advanced Engineering Informatics*, Vol. 28, No. 4, 455–468.
- Cheng T. and Venugopal M. (2011). Performance evaluation of ultra wideband technology for construction resource location tracking in harsh environments, *Automation in Construction*, Vol. 20, No. 8, 1173–1184.
- Decawave Ltd. (2016). EVK1000 user manual, how to use, configure and interface to the dw1000 evaluation kit, Version 1.13.
- Dong Q. and Dargie W. (2012). Evaluation of the reliability of RSSI for indoor localization, In *Proceedings of the 2012 IEEE International Conference on Wireless Communications in Underground and Confined Areas*, Clermont-Ferrand, France, Aug. 28–30, 6 pages.
- Huang Y., Hammad A., and Zhu Z. (2021). Providing proximity alerts to workers on construction sites using Bluetooth Low Energy RTLS, *Automation in Construction*, Vol. 132, 103928.
- Ibrahim M. and Moselhi O. (2014). Automated productivity assessment of earthmoving operations, *Journal of Information Technology in Construction (ITcon)*, Vol. 19, No. 9, 169–184.
- Ibrahim M. (2015). Models for efficient automated site data acquisition, Doctoral dissertation, Concordia University, Montréal, QC, Canada.

- Jo K., Lee M., and Sunwoo M. (2015). Road slope aided vehicle position estimation system based on sensor fusion of GPS and automotive onboard sensors, *IEEE Transactions on Intelligent Transportation Systems*, Vol. 17, No. 1, 250–263.
- Jimenez A. and Seco F. (2016). Comparing decawave and bespoon UWB location systems: Indoor/outdoor performance analysis, In *Proceedings of the 6<sup>th</sup> International Conference of Indoor Positioning Indoor Navigation (IPIN)*, Alcalá de Henares, Spain, Oct. 4–7, 8 pages.
- Kalikova J. and Krcal J. (2017). People counting by means of Wi-Fi, In *Proceedings of the Smart City Symposium (SCSP)*, Prague, Czech Republic, May 25–26, 3 pages.
- Labant S., Gergel'ová M., Weiss G., and Gašinec J. (2017). Analysis of the Use of GNSS Systems in Road Construction, *Proceedings of the IEEE Baltic Geodetic Congress (BGC Geomatics)*, Gdansk, Poland, Jun. 22–25, pp. 72–76.
- Liang P.C. and Krause P. (2015). Smartphone-based real-time indoor location tracking with 1-m precision, *IEEE journal of biomedical and health informatics*, Vol. 20, No. 3, 756–762.
- Li C., Mo L., and Zhang D. (2019). Review on UHF RFID localization methods, *IEEE Journal of Radio Frequency Identification*, Vol. 3, No. 4, 205–215.
- Li H. and Chan G. (2013). Integrating real time positioning systems to improve blind lifting and loading crane operations, *Construction Management and Economics*, Vol. 31, 596–605.
- Li N. and Becerik-Gerber B. (2011). Performance-based evaluation of RFID-based indoor location sensing solutions for the built environment, *Advanced Engineering Informatics*, Vol. 25, No. 3, 535–546.
- Maneesilp J. and Wang C. (2012). RFID support for accurate 3D localization, *IEEE Transactions on Computers*, Vol. 62, No. 7, 1447–1459.
- Masiero A. and Fissore F. (2017). A low cost UWB based solution for direct georeferencing UAV photogrammetry, *Remote Sensing*, Vol. 9, No. 5, paper no. 414.
- Montaser A. and Moselhi O. (2014). RFID indoor location identification for construction projects, *Automation in Construction*, Vol. 39, 167–179.
- Moselhi O. and Bardareh H. (2020). Automated data acquisition in construction with remote sensing technologies, *Applied Sciences*, Vol. 10, No. 8, 2846.
- Motroni A., Buffi A., and Nepa P. (2021). A survey on indoor vehicle localization through RFID technology, *IEEE Access*, Vol. 9, 17921–17942.
- Nurminen H. and Ardeshiri T. (2015). A NLoS-robust TOA positioning filter based on a skew-t measurement noise model, *Proceedings of the International Conference on Indoor Positioning and Indoor Navigation (IPIN)*, Banff, Alberta, Canada, Oct. 13–16, 7 pages.
- Omer M., Ran Y., and Tian G.Y. (2019). Indoor Localization Systems for Passive UHF RFID Tag Based on RSSI Radio Map Database, *Progress in Electromagnetics Research*, Vol. 77, 51–60.
- Park J. and Cho Y.K. (2016). A BIM and UWB integrated mobile robot navigation system for indoor position tracking applications, *Journal of Construction Engineering and Project Management*, Vol. 6, No. 2, 30–39.
- Razavi S.R., Montaser A., and Moselhi O. (2012). RFID deployment protocols for indoor construction, *Construction Innovation*, Vol. 12, No. 2, 239–258.
- Ruiz A.R.J and Granja F.S. (2017). Comparing ubisense, bespoon, and decawave UWB location systems: Indoor performance analysis, *IEEE Transactions on instrumentation and Measurement*, Vol. 66, No. 8, 2106–2117.
- Seo W., Hwang S., Park J., and Lee J.M. (2013). Precise outdoor localization with a GPS–INS integration system, *Robotica*, Vol. 31, No. 3, 371–379.

- Shahi A. and Safa M. (2015). Data fusion process management for automated construction progress estimation, *Journal of Computing in Civil Engineering*, Vol. 29, No. 6, 04014098.
- Siddiqui H. (2014). UWB RTLS for construction equipment localization: experimental performance analysis and fusion with video data, Master's thesis, Institute of Information Systems Engineering, Concordia University, Montréal, QC, Canada.
- Song L. and Tanvir M. (2015). A cost effective material tracking and locating solution for material laydown yard, *Procedia Engineering*, Vol. 123, 538–545.
- Sun M. and Wang Y. (2020). Indoor positioning integrating PDR/geomagnetic positioning based on the genetic-particle filter, *Applied Sciences*, Vol. 10, No. 2, paper no. 668.
- Su X., Li S., Yuan C., Cai H., and Kamat V.R. (2014). Enhanced boundary condition-based approach for construction location sensing using RFID and RTK GPS, *Journal of Construction Engineering and Management*, Vol. 140, No. 10, 04014048.
- Ta V.C. (2017). Smartphone-based indoor positioning using Wi-Fi, inertial sensors and Bluetooth in Machine Learning, Université Grenoble, Alpes, France.
- Technology Solutions (UK) Ltd. (2019). USER guide: 1128 Bluetooth® UHF RFID reader, V. 1.24.
- Tzeng C., Chiang Y., Chiang C., and Lai C. (2008). Combination of radio frequency identification (RFID) and field verification tests of interior decorating materials, *Automation in Construction*, Vol. 18, No. 1, 16–23.
- Valero E., Adán A., and Bosché F. (2016). Semantic 3D reconstruction of furnished interiors using laser scanning and RFID technology, *Journal of Computing in Civil Engineering*, Vol. 30, No. 4, 04015053.
- Wu C., Wang X., Chen M., and Kim M.J. (2019). Differential received signal strength based RFID positioning for construction equipment tracking, *Advanced Engineering Informatics*, Vol. 42, 100960.
- Xu Y. and Shmaliy Y.S. (2018), Robust and accurate UWB-based indoor robot localization using integrated EKF/EFIR filtering, *IET Radar Sonar Navigation*, Vol. 12, 750–756.
- Yoo J. and Park J. (2019). Indoor localization based on Wi-Fi received signal strength indicators: feature extraction, mobile fingerprinting, and trajectory learning, *Applied Sciences*, Vol. 9, No. 18, 3930.
- Zhu Z. and Ren X. (2016). Visual tracking of construction jobsite workforce and equipment with particle filtering, *Journal of Computing in Civil Engineering*, Vol. 30, No. 6, 04016023.